

# Update on non-unitary mixing in the recent NO $\nu$ A and T2K data

Xin Yue Yu, Zishen Guan, Ushak Rahaman,\* and Nikolina Ilic  
*Department of Physics, University of Toronto, Toronto, ON M5S 1A7, Canada*  
(Dated: January 7, 2025)

In this letter, we have used a non-unitary mixing scheme to resolve the tension between NO $\nu$ A and T2K data. It is demonstrated that the results of NO $\nu$ A and T2K can be explained by the effects by non-unitary mixing arising from  $\alpha_{00}$  and  $\alpha_{10}$ . For  $\alpha_{00}$  there is a large overlap between the allowed NO $\nu$ A and T2K regions for NH on the  $\sin^2 \theta_{23} - \delta_{\text{CP}}$  plane at  $1\sigma$ . However, the tension still exists. NO $\nu$ A rules out unitary mixing at a  $3\sigma$  level, whereas T2K strongly prefers unitary mixing. For  $\alpha_{10}$ , the tension can be **well resolved** with the best-fit point for NH at  $|\alpha_{10}| = 0.06$  for both experiments.

**Introduction:** The neutrino oscillation phenomenon, driven by three mixing angles  $\theta_{12}$ ,  $\theta_{13}$  and  $\theta_{23}$ ; two mass squared differences  $\Delta_{21} = m_2^2 - m_1^2$  and  $\Delta_{31} = m_3^2 - m_1^2$ , where  $m_i$ s are the absolute masses of three neutrino mass eigen states  $\nu_i$ s, with  $i = 1, 2, 3$ ; and a CP violating phase  $\delta_{\text{CP}}$ , provides one of the windows to physics beyond the standard model (BSM). The currently unknown properties related to neutrino oscillation physics are the sign of  $\Delta_{31}$ , octant of  $\theta_{23}$ , and the value of  $\delta_{\text{CP}}$ . Depending on the sign of  $\Delta_{31}$ , there can be two different mass hierarchies: normal hierarchy (NH) for  $\Delta_{31} > 0$ ; and inverted hierarchy (IH) for  $\Delta_{31} < 0$ . Similarly, if  $\sin^2 2\theta_{23} < 1$ , there can be two different octants of  $\theta_{23}$ : lower octant (LO) for  $\theta_{23} < \pi/4$ ; and a higher octant (HO) for  $\theta_{23} > \pi/4$ . The present long-baseline accelerator neutrino experiments NO $\nu$ A [1] and T2K [2] are expected to measure these unknowns. However, the 2020 and 2024 data from NO $\nu$ A [3, 4] is in mild tension [5] with the latest T2K data from 2020, [6, 7] for the  $\delta_{\text{CP}}$  measurements and both experiments disfavour each other's  $1\sigma$  allowed regions on the  $\sin^2 \theta_{23} - \delta_{\text{CP}}$  plane. These tensions opened up the possibility of the existence of BSM physics in the NO $\nu$ A and T2K data [8–12]. We have presented our analysis of the latest NO $\nu$ A and T2K data in Appendix B. In this letter, we explore the non-unitary mixing in the NO $\nu$ A and T2K experiment as a possible solution to the tension. This is an update from ref. [9]. Here, we consider one non-unitary parameter at a time, unlike the referenced analysis where all of the parameters simultaneously analyzed. This has allowed us to pinpoint the exact effect of non-unitary parameters responsible for resolving the tension. We also provide a theoretical explanation of our results, based on the effects of different parameters on the oscillation probabilities. Finally, we consider the role of a future combined result of NO $\nu$ A and T2K, and the upcoming long-baseline experiment, DUNE [13], under the assumption that non-unitary mixing exists.

**Non-unitary mixing:** If more than three neutrino generations exist as iso-singlet heavy neutral leptons (HNL), they would not take part in neutrino oscillations

in the minimal extension of the standard model. However, their admixture in charged current weak interactions will affect neutrino oscillation and the neutrino oscillation will be described by an effective  $3 \times 3$  non-unitary mixing matrix. In case of non-unitary mixing, the effective  $3 \times 3$  mixing matrix can be written as [14]:

$$N = N_{NP} U_{3 \times 3} = \begin{bmatrix} \alpha_{00} & 0 & 0 \\ \alpha_{10} & \alpha_{11} & 0 \\ \alpha_{20} & \alpha_{21} & \alpha_{22} \end{bmatrix} U_{\text{PMNS}} \quad (1)$$

where  $U_{\text{PMNS}}$  is the standard  $3 \times 3$  PMNS mixing matrix. The diagonal elements  $\alpha_{ii}$  of  $N_{NP}$  are real, and the off-diagonal elements  $\alpha_{ij} = |\alpha_{ij}| e^{i\phi_{ij}}$  are complex, with  $i, j = 1, 2, 3$  and  $i > j$ . The details of the calculation of the oscillation probability with non-unitary mixing have been discussed in ref. [9]. The present  $3\sigma$  boundary values for non-unitary parameters are given in ref. [15].

In our analysis, we have considered  $\alpha_{00}$ ,  $\alpha_{10}$ , and  $\alpha_{11}$  as the possible source of the non-unitary effect, since these three parameters have the maximum effect on  $P_{\mu e}$  and  $P_{\bar{\mu} \bar{e}}$ , which are the oscillation probabilities for  $\nu_e$  and  $\bar{\nu}_e$  appearances from a  $\nu_\mu$  beam. The details of our analysis are provided in Appendix A.

**Results:** From Fig. 1 it can be seen that for  $\alpha_{00}$ , the two experiments have small overlap at a  $1\sigma$  confidence level (C.L.) for NH. However, NO $\nu$ A loses its  $\delta_{\text{CP}}$  sensitivity when the mass hierarchy is the NH. Both experiments have some allowed values for  $\theta_{23}$  in the LO for both of the hierarchies. The combined analysis has a best-fit point at IH. However, there is a degenerate best-fit point at NH with  $\Delta\chi^2 = 0.21$ . For  $\alpha_{10}$ , the  $1\sigma$  overlap between two experiments for NH is larger. As in the preceding case, NO $\nu$ A loses its  $\delta_{\text{CP}}$  sensitivity for NH. The T2K best-fit point occurs at the IH and with  $\theta_{23}$  in the LO. However, there exist degenerate best-fit points at IH-HO ( $\Delta\chi^2 = 0.74$ ), NH-HO ( $\Delta\chi^2 = 0.72$ ), and NH-LO ( $\Delta\chi^2 = 0.34$ ). From Fig. 2, it can be observed that for the  $\alpha_{00}$  parameter, NO $\nu$ A and the combined analysis rule out unitary-mixing at more than  $3\sigma$  C.L. However T2K alone prefers a best-fit of  $\alpha_{00}$  closer to unitary,  $\alpha_{00} = 1$ , and the unitary mixing case is allowed at  $1\sigma$  C.L. In addition, it can be seen that NO $\nu$ A and T2K rule out each other's best-fit  $\alpha_{00}$  value at more than  $3\sigma$ . However, for the  $\alpha_{10}$  parameter, the results of both

\* ushak.rahaman@cern.ch

experiments are more consistent with each other. Both experiments allow each other's best-fit points for both hierarchies at  $1\sigma$ . For NH, T2K rules out the unitary mixing value  $|\alpha_{10}| = 0$  at more than  $1\sigma$  C.L.

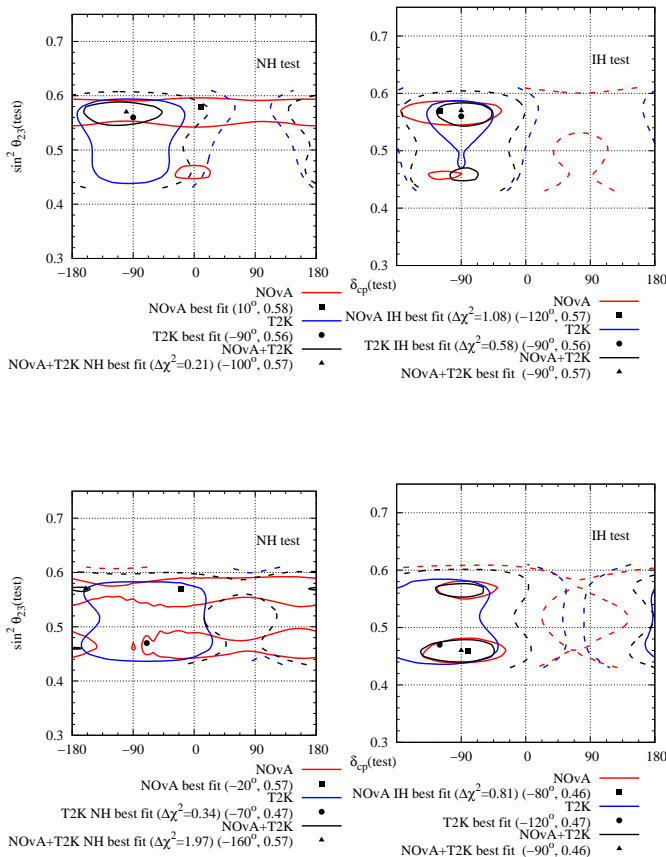


FIG. 1. Allowed regions in the  $\sin^2 \theta_{23} - \delta_{CP}$  plane for  $\text{NO}\nu\text{A}$  and T2K after analysing the data with non-unitary mixing with  $\alpha_{00}$  in the upper (lower) panel. The left (right) panel is for NH (IH). The red (blue) line indicates  $\text{NO}\nu\text{A}$  (T2K), and the black line indicates the combined data. The solid (dotted) lines indicate the boundaries of the  $1\sigma$  ( $3\sigma$ ) allowed regions.

We will explain the results in terms of the effects on  $P_{\mu e}$  and  $P_{\bar{\mu} e}$  due to the changes in oscillation parameters. Following the methodology in ref. [5], we will consider vacuum oscillations, with  $\theta_{23}$  maximal and  $\delta_{CP} = 0$  as our benchmark parameter values and refer to this combination as 000. We have denoted the parameter values responsible for boosting (suppressing)  $P_{\mu e}$  as + (-). For instance, when matter effect is introduced,  $P_{\mu e}$  is increased for NH and decreased for IH. Hence, we have denoted the  $P_{\mu e}$  increase for NH as +, and decrease for IH as -. Similarly, the increase in  $P_{\mu e}$  when  $\theta_{23}$  in the HO (LO) has been denoted as + (-). Finally  $\delta_{CP} = -90^\circ$  ( $90^\circ$ ) corresponds to an increase (decrease) in  $P_{\mu e}$ , and is denoted as + (-). It is to be noted that the effects of hierarchy and  $\delta_{CP}$  on  $P_{\bar{\mu} e}$  are opposite to those on  $P_{\mu e}$ ,

while the effect of the octant choice is similar for both  $P_{\bar{\mu} e}$  and  $P_{\mu e}$ .

At 000 the expected  $\nu_e$  and  $\bar{\nu}_e$  event numbers (signal+background) for  $\text{NO}\nu\text{A}$  are 170 and 33 respectively. The observed  $\nu_e$  and  $\bar{\nu}_e$  event numbers for  $\text{NO}\nu\text{A}$  are 181 and 32 respectively. Therefore,  $\text{NO}\nu\text{A}$  observes a moderate boost in observed  $\nu_e$  event numbers compared to the benchmark point. In case of unitary-mixing, this moderate boost can happen due to the parameter labels: (i)  $++-$ , (ii)  $+ - +$ , and (iii)  $- + +$ . For the current  $\nu_e$  data collected, label candidates that explain the moderate event excesses include  $++-$  and  $- + +$ . As for the  $\bar{\nu}_e$  appearance channel, the observed number of events is consistent with the expected number of events corresponding to the 000 case. However, due to the lack of statistics in the  $\bar{\nu}$  data, all other possible combinations are also allowed, except  $++-$  and  $- + -$ . These two combinations lead to the minimum and maximum number of expected event rates in the  $\bar{\nu}_e$  appearance channels, respectively. Therefore the unitary mixing analysis of the  $\text{NO}\nu\text{A}$  data, in entirety, results in a solution of the form  $++-$  and  $- + +$ .

When non-unitary mixing is introduced through  $\alpha_{00}$ , both  $P_{\mu e}$  and  $P_{\bar{\mu} e}$  for  $\text{NO}\nu\text{A}$  are reduced significantly for  $\alpha_{00} = 0.73$  for NH and  $\alpha_{00} = 0.75$  for IH. Hence, the parameter label  $+++$ , which ensures a large increase in standard  $P_{\mu e}$  due to the three parameters, only results in a moderate increase in case of non-unitary mixing due to  $\alpha_{00}$ . Thus,  $+++$ , becomes a viable parameter combination at the  $1\sigma$  C.L. for  $\text{NO}\nu\text{A}$  when  $\alpha_{00}$  is the source of non-unitary mixing.

The observed  $\nu_e$  and  $\bar{\nu}_e$  event numbers for T2K are 107 and 15 respectively. At 000, the expected event numbers for  $\nu_e$  and  $\bar{\nu}_e$  are 80 and 19 respectively. T2K observes a large excess of  $\nu_e$  events compared to the expected events at the benchmark label. For the NH scenario, T2K receives a 7 – 8% boost to T2K  $\nu_e$  appearance events. A large boost is possible when  $\theta_{23}$  is located in HO, but the disappearance data do not allow  $\sin^2 \theta_{23} > 0.59$ . Since the choice of hierarchy and octant can effect the event numbers by only 20% with respect to the benchmark label 000, T2K  $\nu_e$  appearance data firmly anchors around  $\delta_{CP} = -90^\circ$  for the unitary mixing case.

The introduction of non-unitary mixing through  $\alpha_{00}$  reduces  $P_{\mu e}$ , and hence cannot account for the large boost T2K observes in the  $\nu_e$  appearance event numbers. For NH,  $\sin^2 \theta_{23} = 0.57$ ,  $\delta_{CP} = -90^\circ$  ( $+++$ ), in the case of unitary mixing, the event number gets a maximum boost with respect to the 000 configuration. However, for non-unitary mixing due to  $\alpha_{00}$ , the expected  $\nu_e$  event number for  $\alpha_{00} = 0.79$  (best-fit value of the combined data) at these parameter values is only 77, which is much less than the observed event number. Therefore, T2K prefers  $\alpha_{00} \sim 1$ , and rules out the large non-unitary mixing best-fit  $\alpha_{00}$  value of  $\text{NO}\nu\text{A}$  and of the combined analysis at  $3\sigma$  C.L.

In case of  $\alpha_{10}$ , the effects of  $\alpha_{10}$  on  $P_{\mu e}$  and  $P_{\bar{\mu} e}$  are different for  $\delta_{CP} = -90^\circ$  and  $\delta_{CP} = +90^\circ$ . Hence both

the  $\nu_e$  and  $\bar{\nu}_e$  event numbers face a boost (suppression) for  $\delta_{\text{CP}} = -90^\circ$  ( $90^\circ$ ). At the NO $\nu$ A best-fit value region  $++0$ , the expected number of events are 249 for  $\nu_e$ , and 34 for  $\bar{\nu}_e$ . However, there is a near degenerate solution at  $--+$  with 197 (38) expected  $\nu_e$  ( $\bar{\nu}_e$ ) events. Similarly,  $000$  is also a feasible solution for NO $\nu$ A in case of non-unitary mixing due to  $\alpha_{10}$ . At  $+++$ , although the expected number of  $\nu_e$  events is much larger compared to the observed one, the expected number of  $\bar{\nu}_e$  matches exactly with the observed event numbers, making it allowed at  $1\sigma$ . Similarly  $+- -$  is also allowed at a  $1\sigma$  level.

In case of T2K, the best-fit point is explained by the  $---$  case, with the expected  $\nu_e$  ( $\bar{\nu}_e$ ) events being 108 (19), compared to the observed event number 107 (15). However, there is a near degenerate best-fit at  $+ - +$  with the expected  $\nu_e$  ( $\bar{\nu}_e$ ) events being 115 (17). At the standard best-fit point  $+++$ , the expected 133  $\nu_e$  events is much higher than the observed 107 events, but the proximity of 21 expected  $\bar{\nu}_e$  events to the 19 observed events makes it allowed at  $1\sigma$ . Similarly,  $- + +$  is also allowed at  $1\sigma$ .

A detailed discussion on the effect of  $\alpha_{00}$  and  $\alpha_{10}$  on oscillation probabilities and electron and positron appearance event numbers has been performed and is presented in Appendix C. From the discussion in Appendix C, we can conclude that it would be unwise to say that  $\alpha_{00}$  can resolve the tension. However, the tension can be resolved with non-unitary mixing due to  $\alpha_{10}$ . We analysed the data with non-unitary mixing due to  $\alpha_{11}$  as well and found that the result remain the same as the unitary mixing case.

**Future sensitivity:** We have computed the sensitivity of  $\alpha_{00}$  and  $\alpha_{10}$  in the form of contour plots assuming  $\alpha_{10}$  as the true parameter value. We have considered a combination of future NO $\nu$ A results with  $13.305 \times 10^{21}$  ( $6.25 \times 10^{21}$ ) POTs collected for a  $\nu$  ( $\bar{\nu}$ ) run along with future T2K results with  $9.85 \times 10^{21}$  ( $8.15 \times 10^{21}$ ) POTs collected for a  $\nu$  ( $\bar{\nu}$ ) run. We have also separately considered DUNE with a  $\nu$  and  $\bar{\nu}$  run, each corresponding to  $5.5 \times 10^{21}$  POTs collected. We have presented the result in the form of contour plots in fig. 3 with true values  $|\alpha_{10}|$  on the x-axis and the test values of  $|\alpha_{10}|$  and  $\alpha_{00}$  on the y-axis. To generate these plots, we fixed the true values of standard oscillation parameters at their current global best-fit values given in ref. [16]. The true values of  $|\alpha_{10}|$  have been varied in the range  $[0 : 0.1]$ , with true  $\phi_{10} = 0$ . For test parameters, we varied  $\delta_{\text{CP}}$  in its complete range, while  $\sin^2 \theta_{23}$  and  $|\Delta_{31}|$  have been varied in their current  $3\sigma$  range given in ref. [16]. Other standard parameters' test values have been fixed to their best-fit values. For non-unitary parameters, we varied the test values of  $|\alpha_{10}|$  in the range  $[0 : 0.1]$  and test values of  $\phi_{10}$  in the range  $[-180^\circ : 180^\circ]$ . We marginalised the  $\Delta\chi^2$  over all the test parameters except  $|\alpha_{10}|$ . When  $\alpha_{00}$  is the test parameter, we varied it in the range  $[0.7 : 1]$  and marginalised  $\Delta\chi^2$  over the standard test parameters. It can be seen from fig. 3 that when non-unitary

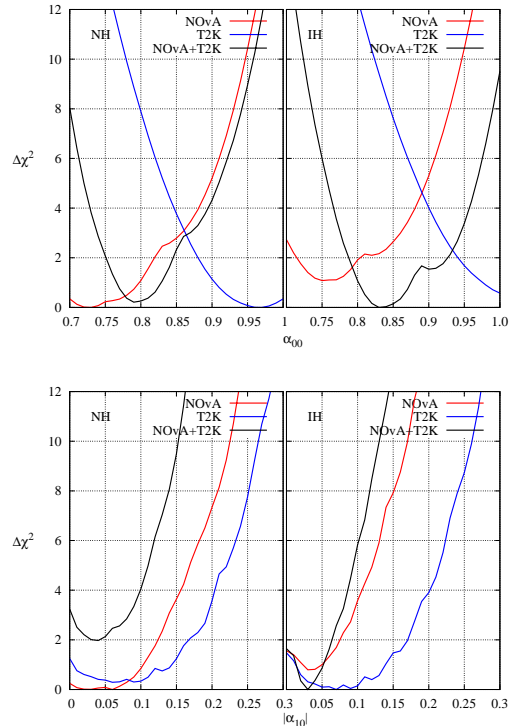


FIG. 2.  $\Delta\chi^2$  as a function of individual non-unitary parameters for 2024 long baseline data.

mixing arises due to  $\alpha_{10}$ , and when true and test hierarchies are the same, the test values of  $|\alpha_{10}|$  can be ruled out at  $1\sigma$  outside the range of the true values within a  $\pm 0.03$  uncertainty by the combination of future NO $\nu$ A and T2K data. A future DUNE run can exclude the test values of  $|\alpha_{10}|$  outside the range of true value within a  $\pm 0.01$  uncertainty. When true and test hierarchies are opposite, then the combination of NO $\nu$ A and T2K rules out regions outside  $0 \leq \alpha_{10}(\text{true}) \leq 0.025$  ( $0.045 < \alpha_{10}(\text{true}) \leq 0.1$ ) and  $0 \leq \alpha_{10}(\text{test}) \leq 0.063$  ( $0 < \alpha_{10}(\text{test}) \leq 0.06$ ) for NH true-IH test (IH true-NH test) at  $3\sigma$  C.L. DUNE rules out the wrong hierarchy at a  $3\sigma$  level. When true and test hierarchies are the same, the combination of a NO $\nu$ A and T2K future run allows for a very small region corresponding to  $0 \leq |\alpha_{10}|(\text{true}) \leq 0.025$  ( $0 \leq |\alpha_{10}|(\text{true}) \leq 0.045$ ) and  $0.92 \leq \alpha_{00}(\text{test}) \leq 1$  ( $0.87 \leq \alpha_{00}(\text{test}) \leq 1$ ) at  $1\sigma$  ( $3\sigma$ ) C.L. The future DUNE run allows for a tiny region close to  $|\alpha_{10}|(\text{true}) = 0$  and  $\alpha_{00}(\text{test}) = 1$  at a  $1\sigma$  C.L. At  $3\sigma$ , DUNE allows for  $0 \leq |\alpha_{10}|(\text{true}) \leq 0.03$  and test  $0.95 \leq \alpha_{00}(\text{test}) \leq 1$ . When NH is the true hierarchy, the future combination of NO $\nu$ A and T2K results, as well as DUNE can rule out an IH test at  $3\sigma$  level, for a  $\alpha_{00}(\text{test})$ . When IH is the true hierarchy, the combination of NO $\nu$ A and T2K results rule out the NH test outside the range  $0 \leq |\alpha_{10}|(\text{true}) \leq 0.04$  and  $0.95 \leq \alpha_{00}(\text{test}) \leq 1$  at  $3\sigma$ . DUNE rules out the NH test completely at  $3\sigma$ .

**Conclusion:** The tension between NO $\nu$ A and T2K

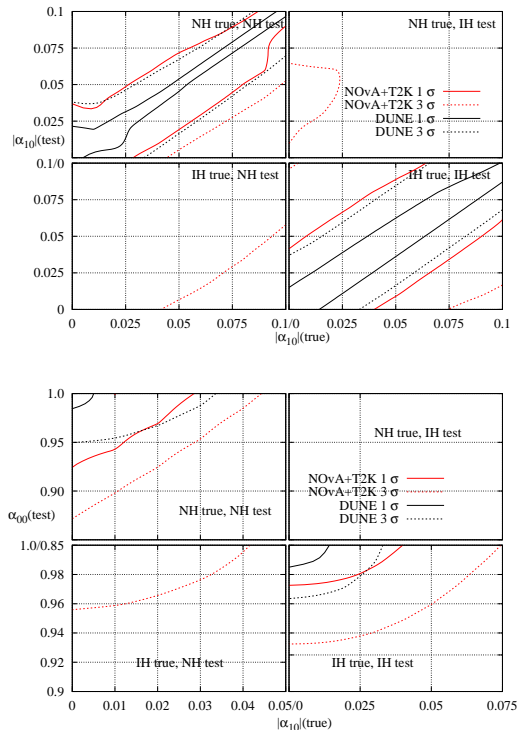


FIG. 3. Sensitivity of  $|\alpha_{10}|$  and  $\alpha_{00}$  assuming  $\alpha_{10}$  as the true parameter for future combination of  $\text{NO}\nu\text{A}$  and T2K, and DUNE.

arises from the  $\nu_e$  appearance channel.  $\text{NO}\nu\text{A}$  observed a moderate excess in its electron appearance event number compared to the expected event numbers for the

benchmark parameter values, namely vacuum oscillation,  $\theta_{23}$  maximal and  $\delta_{\text{CP}} = 0$ . This moderate excess can be accommodated with the combination of NH,  $\theta_{23}$  in HO,  $0 < \delta_{\text{CP}} < 180^\circ$  and IH,  $\theta_{23}$  in HO, and  $-180^\circ < \delta_{\text{CP}} < 0$ . On the other hand, T2K observes a large excess in the observed electron event numbers, compared to the benchmark point. This large excess can only be accommodated with  $\delta_{\text{CP}}$  firmly anchored around  $-90^\circ$ . This gives rise to the tension at NH. A combination of the two experiments prefers IH over NH. When non-unitary mixing is introduced through  $\alpha_{00}$ , the  $\nu_\mu \rightarrow \nu_e$  and  $\bar{\nu}_\mu \rightarrow \bar{\nu}_e$  oscillation probabilities face a suppression for all of the combinations of standard oscillation parameter values. This suppression makes NH,  $\theta_{23}$  in HO and  $-180^\circ < \delta_{\text{CP}} < 0$  a viable explanation for the  $\text{NO}\nu\text{A}$  results, making its allowed region on the  $\sin^2 \theta_{23} - \delta_{\text{CP}}$  plane overlap with that of T2K for NH. However, because of this suppression, non-unitary mixing cannot account for the large excess in T2K  $\nu_e$  appearance event number, and hence T2K strongly prefers unitary mixing. In the case of  $\alpha_{10}$  being the reason for non-unitary mixing, the  $\nu_e$  appearance events of both the experiments see a boost (suppression) for  $\delta_{\text{CP}} = -90^\circ$  ( $90^\circ$ ) for both the hierarchies and octants of  $\theta_{23}$ . Thus, in this case,  $\theta_{23}$  in LO becomes a viable solution for both experiments. In this case, both experiments have large overlap between the allowed regions at  $1\sigma$  on the  $\sin^2 \theta_{23} - \delta_{\text{CP}}$  plane. Both experiment have a preference for non-unitary mixing with best-fit point at  $|\alpha_{10}| = 0.06$  for NH.  $\alpha_{11}$  does not have any effect on the results of  $\text{NO}\nu\text{A}$  and T2K. The future run of  $\text{NO}\nu\text{A}$  and T2K have good potential to rule out the wrong values of  $|\alpha_{10}|$  as well as  $\alpha_{00}$  if non-unitary mixing arises due to  $\alpha_{10}$ . The sensitivity is improved by future DUNE data.

- 
- [1] D. S. Ayres et al. ( $\text{NO}\nu\text{A}$ ) (2007).  
[2] Y. Itow et al. (T2K), in *3rd Workshop on Neutrino Oscillations and Their Origin (NOON 2001)* (2001), pp. 239–248, hep-ex/0106019.  
[3] M. A. Acero et al. ( $\text{NO}\nu\text{A}$ ) (2021), 2108.08219.  
[4] J. Wolcott, *New oscillation results from nova with 10 years of data* (2024), talk given at the Neutrino 2024 meeting on June, 17th, 2024, URL <https://agenda.infn.it/event/37867/contributions/233955/attachments/217832/177712/2024-06-17%20Wolcott%20NOvA%202024.pdf>.  
[5] U. Rahaman and S. K. Raut, Eur. Phys. J. C **82**, 910 (2022), 2112.13186.  
[6] K. Abe et al. (T2K Collaboration), Phys.Rev.Lett. **112**, 061802 (2014), 1311.4750.  
[7] K. Abe et al. (T2K Collaboration), Phys.Rev.Lett. **112**, 181801 (2014), 1403.1532.  
[8] U. Rahaman (2021), 2103.04576.  
[9] L. S. Miranda, P. Pasquini, U. Rahaman, and S. Razaque, Eur. Phys. J. C **81**, 444 (2021), 1911.09398.  
[10] S. S. Chatterjee and A. Palazzo, Phys. Rev. Lett. **126**, 051802 (2021), 2008.04161.  
[11] U. Rahaman, S. Razaque, and S. U. Sankar, Universe **8**, 109 (2022), 2201.03250.  
[12] S. S. Chatterjee and A. Palazzo (2024), 2409.10599.  
[13] B. Abi et al. (DUNE) (2018), 1807.10334.  
[14] F. J. Escrihuela, D. V. Forero, O. G. Miranda, M. Tortola, and J. W. F. Valle, Phys. Rev. **D92**, 053009 (2015), [Erratum: Phys. Rev.D93,no.11,119905(2016)], 1503.08879.  
[15] F. J. Escrihuela, D. V. Forero, O. G. Miranda, M. Tortola, and J. W. F. Valle, New J. Phys. **19**, 093005 (2017), 1707.02132.  
[16] I. Esteban, M. C. Gonzalez-Garcia, M. Maltoni, I. Martinez-Soler, J. a. P. Pinheiro, and T. Schwetz (2024), 2410.05380.  
[17] Y. Itow et al. (T2K), pp. 239–248 (2001), hep-ex/0106019.  
[18] D. Ayres et al. ( $\text{NO}\nu\text{A}$ ), Tech. Rep. (2007), FERMILAB-DESIGN-2007-01.  
[19] I. Esteban, M. C. Gonzalez-Garcia, A. Hernandez-Cabezudo, M. Maltoni, and T. Schwetz, JHEP **01**, 106 (2019), 1811.05487.  
[20] P. Huber, M. Lindner, and W. Winter, Comput.Phys.Commun. **167**, 195 (2005), hep-ph/0407333.

## Appendix A: Analysis details

The T2K experiment [17] uses the  $\nu_\mu$  beam from the J-PARC accelerator at Tokai and the water Cherenkov detector at Super-Kamiokande, which is 295 km away from the source. The detector is situated  $2.5^\circ$  off-axis. The flux peaks at 0.7 GeV, which is also close to the first oscillation maximum. T2K started taking data in 2009 and up until 2020 released results [6, 7] corresponding to  $1.97 \times 10^{21}$  ( $1.63 \times 10^{21}$ ) protons on target (POTs) in neutrino (anti-neutrino) mode.

The NO $\nu$ A detector [18] is a 14 kt totally active scintillator detector (TASD), placed 810 km away from the neutrino source at Fermilab, situated  $0.8^\circ$  off-axis with respect to the NuMI beam. The flux peaks at 2 GeV, close to the oscillation maxima at 1.4 GeV (1.8 GeV) for NH (IH). NO $\nu$ A started taking data in 2014 and as of the 2024 data release [4], has collected  $2.661 \times 10^{21}$  ( $1.250 \times 10^{21}$ ) POTss, for neutrino (anti-neutrino) mode.

Since the T2K data are from 2020, in order to analyze the data from both of the experiments, we have used the 2019 global-best fit values for standard oscillation parameters [19]. We have fixed  $\Delta_{21}$  and  $\theta_{12}$  to their best-fit values. The values of  $\sin^2 \theta_{13}$ ,  $\sin^2 \theta_{23}$  and  $\Delta_{3l}$ , with  $l = 1$  (2) for NH (IH) have been varied in their  $3\sigma$  range.  $\delta_{CP}$  has been varied in its complete range  $[-180^\circ : 180^\circ]$ . Among the non-unitary parameters,  $\alpha_{00}$  and  $\alpha_{11}$  have been varied within the range  $[0.7 : 1.0]$ , while  $|\alpha_{10}|$  has been varied within the range  $[0 : 0.3]$ , and  $\phi_{10}$  has been allowed to take on any value  $[-180^\circ : 180^\circ]$ . We have chosen these ranges to cover the  $3\sigma$  regions given in ref. [9]. We have used GLoBES [20] to calculate the theoretical event rates as well as the  $\chi^2$  between theoretical event rates and experimental data. To do so, we fixed the bin based detector efficiencies by matching with the simulated event numbers provided by NO $\nu$ A [4] and T2K collaborations [6, 7]. For energy resolution, we used a Gaussian function

$$R^c(E, E') = \frac{1}{\sqrt{2\pi}} e^{-\frac{(E-E')^2}{2\sigma^2(E)}}, \quad (\text{A1})$$

where  $E'$  is the reconstructed energy. The energy resolution function is given by

$$\sigma(E) = \alpha E + \beta\sqrt{E} + \gamma, \quad (\text{A2})$$

where  $\alpha = 0$ ,  $\beta = 0.075$ ,  $\gamma = 0.05$  for T2K. For NO $\nu$ A, however, we used  $\alpha = 0.11$  (0.09),  $\beta = \gamma = 0$  for  $\nu_e$  ( $\nu_\mu$ ) events. For systematics uncertainty, we have used 5% energy calibration and flux normalization backgrounds for both of the experiments. The experimental event rates have been taken from ref. [6, 7] for T2K, and [4] for NO $\nu$ A.

## Appendix B: Analysis of NO $\nu$ A and T2K data with unitary mixing scheme

In this section, we present the analysis, with standard unitary mixing scheme, of NO $\nu$ A and T2K latest data. From fig. 4, it can be seen that the best-fit points of the two experiments are far apart from each other. There are no overlaps between the  $1\sigma$  allowed regions of the two experiments for NH. Both experiments have their best-fit points at NH. However, T2K has a near degenerate best-fit point at IH. The combined analysis prefers IH over NH. Only a small area near the  $\delta_{CP}$  conserving values at NH are allowed at  $1\sigma$ .

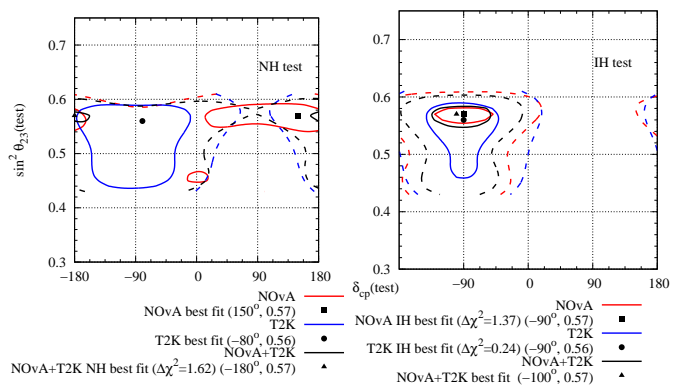


FIG. 4. Allowed regions in the  $\sin^2 \theta_{23} - \delta_{CP}$  plane for NO $\nu$ A and T2K after analysing the data with standard unitary mixing. The left (right) panel is for NH (IH). The red (blue) line indicates NO $\nu$ A (T2K), and the black line indicates the combined data. The solid (dotted) lines indicate the boundaries of the  $1\sigma$  ( $3\sigma$ ) allowed regions.

## Appendix C: Oscillation probabilities and event numbers of NO $\nu$ A and T2K

In this section, we will discuss the effect of non-unitary mixing due to  $\alpha_{00}$  and  $\alpha_{10}$  on oscillation probabilities  $P_{\mu e}$  and  $P_{\bar{\mu} \bar{e}}$  as well as the  $\nu_e$  and  $\bar{\nu}_e$  event numbers. In figs. 5, we have shown the oscillation probabilities  $P_{\mu e}$  and  $P_{\bar{\mu} \bar{e}}$  as a function of neutrino energy in the left and right panels respectively for different hierarchy and  $\delta_{CP}$  values and for both unitary and non-unitary mixing due to  $\alpha_{00}$ . The top (bottom) panel shows the oscillation probabilities for NO $\nu$ A (T2K). Other parameter values have been fixed at the best-fit point of the combined analysis of NO $\nu$ A and T2K. As we can see that both  $P_{\mu e}$  and  $P_{\bar{\mu} \bar{e}}$  get a strong suppression in case of non-unitary mixing effect due to  $\alpha_{00}$  for all the different hierarchy combinations. This is true for both the experiments.

In fig. 6, we have shown  $P_{\mu e}$  and  $P_{\bar{\mu} \bar{e}}$  as a function of energy for NO $\nu$ A experiment and for different hierarchy- $\delta_{CP}$  combinations. The left (right) panels are for neutrino

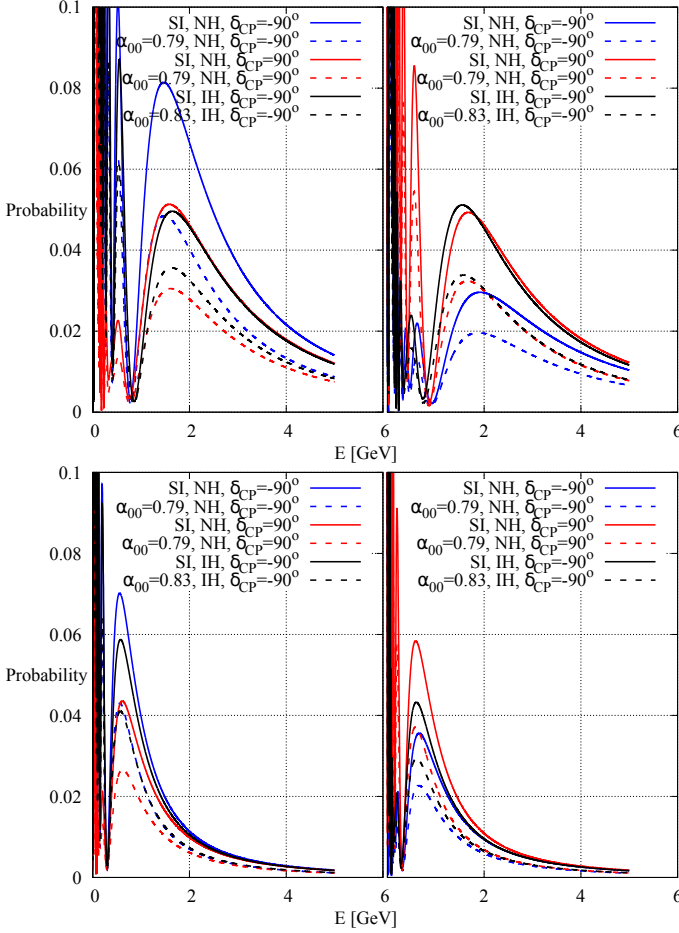


FIG. 5.  $\nu_\mu \rightarrow \nu_e$  (left panel) and  $\bar{\nu}_\mu \rightarrow \bar{\nu}_e$  (right panel) oscillation probability as a function of energy with different hierarchy- $\delta_{CP}$  combinations for standard oscillation and non-unitary mixing due to  $\alpha_{00}$ . The oscillation parameter values including  $\alpha_{00}$  are fixed to the combined best-fit values of NO $\nu$ A and T2K. The top (bottom) panel represents oscillation probabilities for NO $\nu$ A (T2K).

(anti-neutrino), and the top (bottom) panels are for  $\theta_{23}$  in HO (LO). We have used  $\sin^2 \theta_{23} = 0.57$  and  $0.43$  for HO and LO respectively. Other parameters including  $|\alpha_{10}|$  and  $\phi_{10}$  have been fixed at the combined best-fit points of NO $\nu$ A and T2K. As can be seen, in case of non-unitary mixing due to  $\alpha_{10}$ , both  $P_{\mu e}$  and  $P_{\bar{\mu} \bar{e}}$  gets a slight boost at the oscillation peak energy compared to probabilities due to standard unitary mixing. However, for NH- $\delta_{CP} = 90^\circ$  and IH- $\delta_{CP} = -90^\circ$ ,  $P_{\mu e}$  gets a moderate suppression after the oscillation maximum energy compared to the oscillation probabilities due to unitary mixing. In case of anti-neutrino, this suppression after the oscillation maximum energy takes place in case of NH- $\delta_{CP} = -90^\circ$ . This feature remains same for both the octants of  $\theta_{23}$ . In fig. 7, we have shown the similar probability plots for T2K experiment, and we can see the similar features for T2K as well.

In the next step, we have shown the change in expected total (signal+background) event numbers for  $\nu_e$  and  $\bar{\nu}_e$  appearance due to the change in oscillation parameters

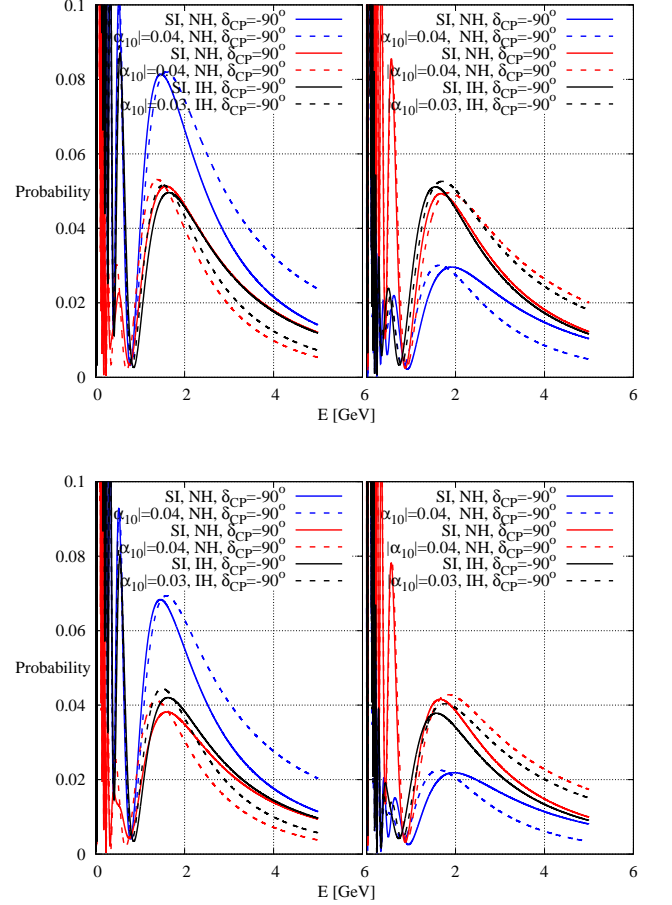


FIG. 6.  $\nu_\mu \rightarrow \nu_e$  (left panel) and  $\bar{\nu}_\mu \rightarrow \bar{\nu}_e$  (right panel) oscillation probability as a function of energy with different hierarchy- $\delta_{CP}$  combinations for standard oscillation and non-unitary mixing due to  $\alpha_{10}$  for the NO $\nu$ A experiment. The oscillation parameter values including  $|\alpha_{10}|$  are fixed to the combined best-fit values of NO $\nu$ A and T2K. For NH (IH),  $\phi_{10} = 120^\circ$  ( $60^\circ$ ). The left (right) panels are for neutrino (anti-neutrino) probabilities, and the top (bottom) panels are for  $\theta_{23}$  in HO (LO). For HO (LO), we have used  $\sin^2 \theta_{23} = 0.57$  ( $0.43$ ).

from the benchmark parameter values of vacuum oscillation,  $\sin^2 \theta_{23} = 0.5$  and  $\delta_{CP} = 0$ -labeled as 000. In table I, we can see that at the benchmark point 000, the expected event numbers for the current NO $\nu$ A POTs are 170 for  $\nu_e$  appearance and 33 for  $\bar{\nu}_e$  events in case of unitary mixing. The observed event numbers are 181 and 33. Therefore, for standard unitary mixing, 000 is a good solution for  $\bar{\nu}_e$  appearance. However, it cannot provide a solution for  $\nu_e$  appearance events. In case of non-unitary mixing due to  $\alpha_{00}$  ( $\alpha_{10}$ ), because of the suppression (boost) in the oscillation probabilities as explained before, the expected number of  $\nu_e$  and  $\bar{\nu}_e$  events are 126 (198) and 24 (35) respectively. Hence, in case of  $\alpha_{10}$ , 000 provides a solution within  $1\sigma$  for both  $\nu_e$  and  $\bar{\nu}_e$  events. But 000 cannot provide a solution for either cases when non-unitary mixing arises from  $\alpha_{00}$ . In table I, the expected event numbers with non-unitary mixing due to

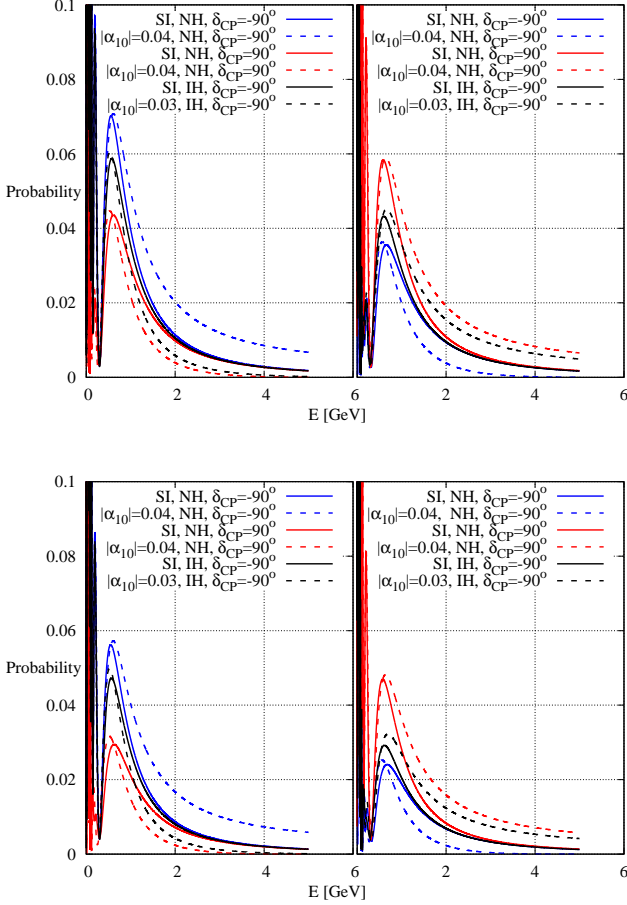


FIG. 7.  $\nu_\mu \rightarrow \nu_e$  (left panel) and  $\bar{\nu}_\mu \rightarrow \bar{\nu}_e$  (right panel) oscillation probability as a function of energy with different hierarchy- $\delta_{\text{CP}}$  combinations for standard oscillation and non-unitary mixing due to  $\alpha_{10}$  for the T2K experiment. The oscillation parameter values including  $|\alpha_{10}|$  are fixed to the combined best-fit values of  $\text{NO}\nu A$  and T2K. For NH (IH),  $\phi_{10} = 120^\circ$  ( $60^\circ$ ). The left (right) panels are for neutrino (anti-neutrino) probabilities, and the top (bottom) panels are for  $\theta_{23}$  in HO (LO). For HO (LO), we have used  $\sin^2 \theta_{23} = 0.57$  (0.43).

$\alpha_{00}$  ( $\alpha_{10}$ ) are given inside parenthesis (square bracket). Next, we changed one parameter at a time and calculated the expected total  $\nu_e$  and  $\bar{\nu}_e$  event numbers for each case. Following the formalism in the main text, we can see that in case of unitary mixing, the closest solution for  $\nu_e$  appearance events are  $++-$  and  $-++$ . Due to the lack of statistics, every possible parameter combination, except  $+ - +$  and  $- + -$ , can provide a solution for  $\bar{\nu}_e$  appearance events at  $1\sigma$  for unitary mixing. These two exceptions account for the minimum and maximum expected  $\bar{\nu}_e$  event numbers for  $\text{NO}\nu A$  in case of unitary mixing. When, non-unitary is introduced through  $\alpha_{00}$  and the oscillation probabilities  $P_{\mu e}$  and  $P_{\bar{\mu} e}$  get a large suppression for all the parameter combinations, the best solution for  $\nu_e$  appearance event number is provided by  $+++$  with expected event number 167 for  $\alpha_{00} = 0.79$ . However, at this point, the expected  $\bar{\nu}_e$  event number is

21, which is much less than the observed  $\bar{\nu}_e$  event number 21. The possible solution for  $\bar{\nu}_e$  event number in case of non-unitary mixing due to  $\alpha_{00}$  are:  $++-$ ,  $-++$ ,  $-+-$ , and  $---$ . However, for the last two parameter combinations:  $-+-$  and  $---$ , the expected number of  $\nu_e$  event numbers are much less compared to the observed ones. Hence the analysis of neutrino and anti-neutrino appearance events at  $\text{NO}\nu A$ , along with the disappearance events, the  $1\sigma$  allowed regions include  $+++$ ,  $++-$ , and  $-++$ .

In case of non-unitary mixing due to  $\alpha_{10}$ , the expected  $\nu_e$  and  $\bar{\nu}_e$  appearance events get a boost (suppression) for  $\delta_{\text{CP}} = -90^\circ$  ( $90^\circ$ ) compared to those for unitary mixing for both the hierarchies and octants. At the benchmark point 000, also both  $P_{\mu e}$  and  $P_{\bar{\mu} e}$  get a boost from non-unitary mixing, making the expected  $\nu_e$  and  $\bar{\nu}_e$  events at 000 as 198 and 35 respectively. Thus, 000 provides a solution at  $1\sigma$  for both  $\nu_e$  and  $\bar{\nu}_e$  appearance events. The other possible solutions at  $1\sigma$  for  $\nu_e$  are  $++-$  and  $-++$ . In case of anti-neutrino, all the parameter combinations, except  $-++$ , provide the possible solutions at  $1\sigma$ . analysing both  $\nu_e$  and  $\bar{\nu}_e$  appearance data, along with the disappearance data,  $1\sigma$  allowed regions are:  $+++$ ,  $++-$ ,  $+--$ ,  $+ - 0$ , and  $- - +$ . A small region in  $-++$  is also allowed at  $1\sigma$  for 2 degrees of freedom.

In case of T2K, as can be seen in table II, the expected number of events at 000 are 79 and 19 respectively for  $\nu_e$  and  $\bar{\nu}_e$  appearance. The observed number of events for these two are 107 and 15 respectively. Thus, T2K observed a large (moderate) boost (suppression) in observed  $\nu_e$  ( $\bar{\nu}_e$ ) events compared to the expectation at the benchmark point. This large boost at T2K can only be accommodated by unitary mixing, when  $\delta_{\text{CP}}$  is firmly anchored around  $\delta_{\text{CP}} = -90^\circ$ . Hence the best possible solution is provided by  $+++$ .  $-++$  can also provide a solution allowed at  $1\sigma$ . In case of non-unitary mixing from  $\alpha_{00}$ , due to the suppression to oscillation probability, none of the parameter combinations can provide any good solution. Hence, T2K strongly prefers unitary mixing as shown in the top panel of fig. 2. When non-unitary mixing arises due to  $\alpha_{10}$ , the expected  $\nu_e$  appearance event number at 000 is 92. Thus 000 is a possible solution at  $1\sigma$ . The best possible solutions are at  $++0$   $- - +$  with 107 and 108 expected event numbers respectively. This is also a possible solution for  $\nu_e$  appearance event at  $\text{NO}\nu A$ . The other possible solutions are  $+00$  and  $+ - +$ . For anti-neutrino, every parameter combination is allowed at  $1\sigma$ . Thus the analysis of total data prefers  $- - +$  as the new best-fit point. The allowed regions at  $1\sigma$  consist of  $-++$ ,  $+ - +$ ,  $+++$ , and  $++0$ .

In the next step, we have emphasized our results with bi-event plots in fig. 8. For this, we calculated the expected  $\nu_e$  and  $\bar{\nu}_e$  event numbers (signal+background) for the current POTs of  $\text{NO}\nu A$  and T2K. To do this, we varied  $\delta_{\text{CP}}$  in the range  $[-180^\circ : 180^\circ]$ . All other oscillation parameters have been fixed at the NH best-fit point of the combined analysis. In this case, the  $\bar{\nu}_e$  vs  $\nu_e$  plot takes el-

liptical shape. In fig. 8, the left and right panel show the bi-event plots for  $\text{NO}\nu\text{A}$  and T2K respectively. The black ellipses indicate standard unitary mixing scheme, while the blue (red) ellipses indicate non-unitary mixing due to  $\alpha_{00}$  ( $\alpha_{10}$ ). The best-fit points indicated on the plots are the combined best-fit points. We can see that in case of  $\alpha_{00}$ , the bi-event plots for both  $\text{NO}\nu\text{A}$  and T2K go farther away from the observed event numbers. However, for  $\text{NO}\nu\text{A}$  the expected  $\nu_e$  event number at the combined best-fit point in case of non-unitary mixing due to  $\alpha_{00}$  is closer to the observed  $\nu_e$  event number. For T2K, at the combined best-fit point, the expected event numbers for both  $\nu_e$  and  $\bar{\nu}_e$  are farther away from the observed event number, compared to the standard case. In the case of  $\alpha_{10}$ , some parts of the bi-event ellipses for both the experiments are closer to the observed event numbers, in comparison to the standard unitary case. Also, at the combined best-fit point, in case of  $\text{NO}\nu\text{A}$  (T2K), the expected  $\nu_e$  (both  $\nu_e$  and  $\bar{\nu}_e$ ) event numbers are closer to the observed event numbers than they are for unitary mixing scheme. The above discussion further emphasizes our conclusion that the tension can be resolved if there is non-unitary mixing due to  $\alpha_{10}$ .

Hierarchy- $\sin^2 \theta_{23}$ - $\delta_{\text{CP}}$	Label	$\nu_e$ Appearance events	$\bar{\nu}_e$ Appearance events
Vacuum-0.5-0	000	170.18(125.95) [197.65]	32.97(23.74) [34.77]
NH-0.5-0	+00	194.11(137.64) [225.90]	28.72(21.67) [30.87]
NH-0.57-0	++0	216.40(152.78) [249.16]	32.01(24.08) [34.26]
NH-0.43-0	+ - 0	186.65(137.37) [217.25]	27.78(21.59) [29.82]
NH-0.57- $-90^\circ$	+++	240.50(167.14) [268.88]	27.05(20.94) [32.17]
NH-0.57- $+90^\circ$	++-	183.98(132.78) [165.16]	34.98(26.02) [30.52]
NH-0.43- $-90^\circ$	+ - +	210.43(151.51) [239.25]	22.84(18.14) [27.70]
NH-0.43- $+90^\circ$	+ - -	153.91(117.15) [136.89]	30.77(23.53) [26.47]
IH-0.57- $-90^\circ$	- ++	182.61(146.77) [216.10]	34.94(26.36) [44.50]
IH-0.43- $-90^\circ$	- - +	163.56(134.26) [197.14]	28.97(22.63) [37.52]
IH-0.57- $+90^\circ$	- + -	138.47(115.57) [121.64]	44.92(33.14) [35.37]
IH-0.43- $+90^\circ$	- - -	119.42(103.07) [104.42]	38.96(29.41) [30.35]

TABLE I. Expected  $\nu_e$  and  $\bar{\nu}_e$  appearance events of  $\text{NO}\nu\text{A}$  for  $2.661 \times 10^{21}$  ( $1.25 \times 10^{21}$ ) POTs in  $\nu$  ( $\bar{\nu}$ ) mode and for different combinations of the unknown parameter values for unitary mixing and non-unitary mixing. The expected event numbers for non-unitary mixing due to  $\alpha_{00} = 0.79$  (0.83) for NH (IH) have been given inside (). The expected event numbers for non-unitary mixing due to  $|\alpha_{10}| = 0.03$  (0.04) and  $\phi_{10} = 120^\circ$  ( $60^\circ$ ) for NH (IH) have been given inside []. The observed numbers of  $\nu_e$  and  $\bar{\nu}_e$  events are 181 and 32 respectively.

Hierarchy- $\sin^2 \theta_{23}$ - $\delta_{\text{CP}}$	Label	$\nu_e$ Appearance events	$\bar{\nu}_e$ Appearance events
Vacuum-0.5-0	000	79.43(57.10) [91.67]	19.04(14.04) [20.71]
NH-0.5-0	+00	84.86(59.80) [97.87]	18.27(13.66) [19.97]
NH-0.57-0	++0	93.77(65.37) [107.21]	19.85(14.36) [21.70]
NH-0.43-0	+ - 0	76.91(55.17) [89.44]	16.69(12.66) [18.20]
NH-0.57- $-90^\circ$	+++	113.32(77.39) [132.79]	17.55(13.21) [20.46]
NH-0.57- $+90^\circ$	++-	77.42(55.20) [66.08]	22.20(16.16) [19.22]
NH-0.43- $-90^\circ$	+ - +	96.45(67.19) [114.47]	14.39(11.20) [16.88]
NH-0.43- $+90^\circ$	+ - -	60.55(45.00) [51.55]	19.04(14.16) [16.36]
IH-0.57- $-90^\circ$	- ++	98.87(75.28) [123.25]	19.15(14.88) [23.73]
IH-0.43- $-90^\circ$	- - +	85.50(65.71) [107.82]	15.10(12.40) [19.36]
IH-0.57- $+90^\circ$	- + -	66.25(52.60) [54.32]	24.56(18.57) [19.99]
IH-0.43- $+90^\circ$	- - -	52.48(43.02) [43.30]	20.91(16.08) [16.91]

TABLE II. Expected  $\nu_e$  and  $\bar{\nu}_e$  appearance events of T2K for  $1.97 \times 10^{21}$  ( $1.63 \times 10^{21}$ ) POTs in  $\nu$  ( $\bar{\nu}$ ) mode and for different combinations of the unknown parameter values for unitary mixing and non-unitary mixing. The expected event numbers for non-unitary mixing due to  $\alpha_{00} = 0.79$  (0.83) for NH (IH) have been given inside (). The expected event numbers for non-unitary mixing due to  $|\alpha_{10}| = 0.03$  (0.04) and  $\phi_{10} = 120^\circ$  ( $60^\circ$ ) for NH (IH) have been given inside []. The observed numbers of  $\nu_e$  and  $\bar{\nu}_e$  events are 107 and 15 respectively.



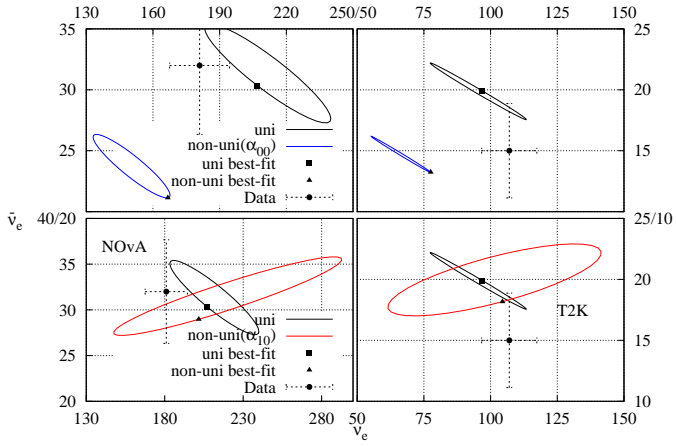


FIG. 8. Bi-event plots for NO $\nu$ A (left) and T2K (right).  $\delta_{CP}$  has been varied in the range  $[-180^\circ : 180^\circ]$ . All other parameters have been fixed at the best-fit values for NH of the combined analysis. The black ellipse marks the case for Standard unitary mixing, while the blue (red) ellipse signifies the non-unitary mixing due to  $\alpha_{00}$  ( $\alpha_{10}$ ). The indicated best-fit points on the plot denote the best-fit point of the combined analysis.